Supplementary information

Optogenetics-integrated gut organ culture system connects enteric neurons dynamics and gut homeostasis

Gitali Naim [1,2,#], Hadar Romano-Zadaka [1,2,#], Sivan Amidror [1,2,#], David Jessula Levy [1,2], Adva Cohen [1,2], Carmel Sochen [3], Hadar Gilberg [1,2], Nairouz Farah [1,2], Vladislav Rudenko [3], Yasmin Yarden [4], Mengyang Feng [4], Rotem Tsentsarevsky [1,2], Ziv Brodie [1,2], Yasmin Reich [1,2], Ariel Simon [1,2], Einat Toister [1,2], Irit Shoval [1], Leah Armon [1], Maya Schiller [5], Yossi Mandel [1,2], Moshe Biton [3], and Nissan Yissachar [1,2,*]

[1] The Goodman Faculty of Life Sciences, Bar-Ilan University, Ramat-Gan, 5290002, Israel.
[2] Bar-Ilan Institute of Nanotechnology and Advanced Materials, Bar-Ilan University, Ramat-Gan, 5290002, Israel.
[3] Department of Immunology and Regenerative Biology, Weizmann Institute of Science, 234 Herzl Street, Rehovot, 7610001, Israel
[4] The Picower Institute for Learning and Memory, Department of Brain and Cognitive Sciences, Massachusetts Institute of Technology, Cambridge, MA 02139, USA
[5] Department of Neurology, The Chaim Sheba Medical Center, Ramat Gan, Israel
[#] These authors contributed equally to this work.
[*] Correspondence: nissan.yissachar@biu.ac.il (N.Y.).

This file contains Supplementary Figures 1-9

Supplementary figure 1

a

Assembly instruction

Bottom
An opaque gut culture device

Middle
Intermediate gas mixture input

Top
The Arduino UNO, a microcontroller board

A three-layer device

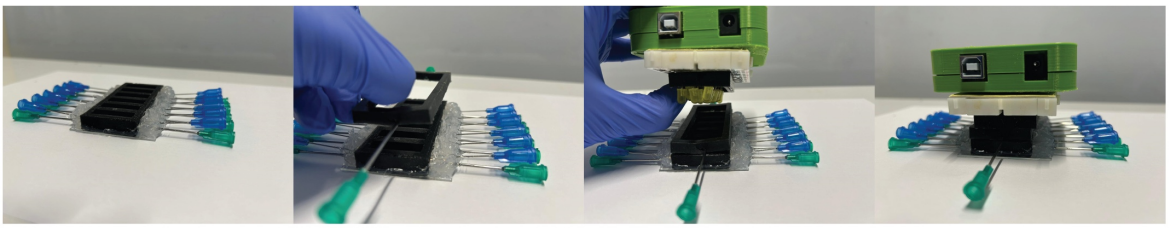

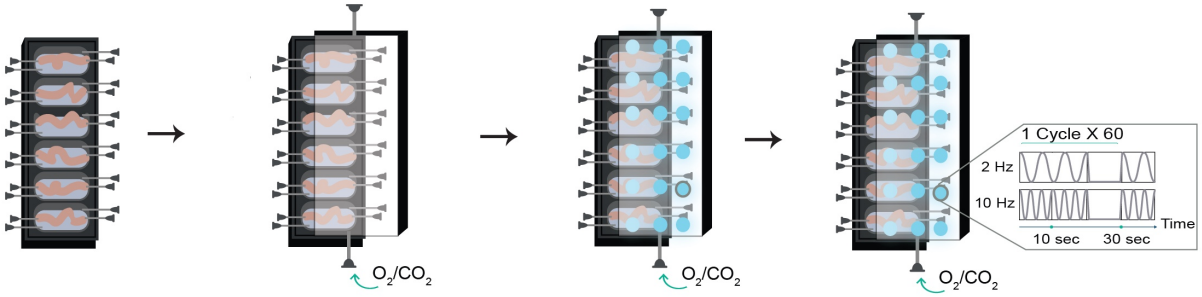

b

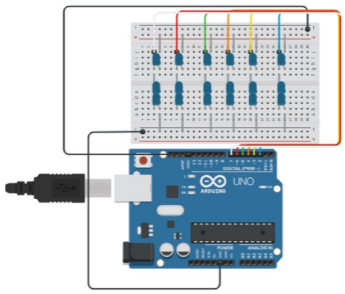

c

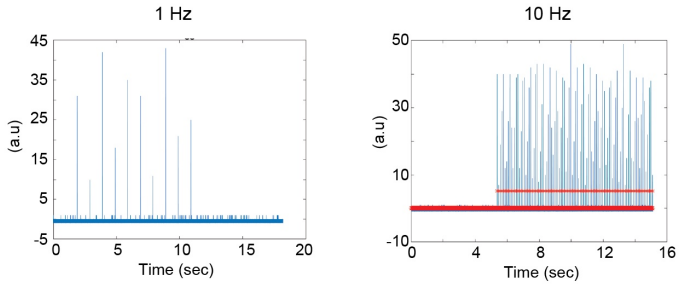

d

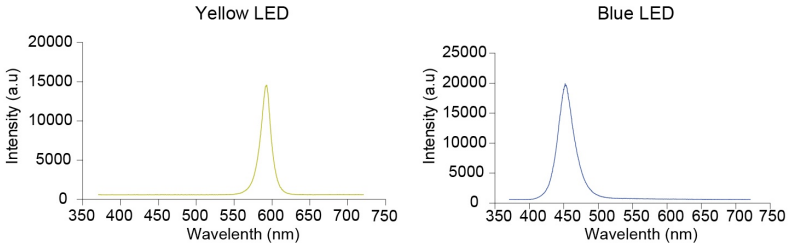

Supplementary Fig. 1: Assembly and validation of the optogenetics-integrated gut organ culture system.

(a) Stepwise assembly of the three-layer culture device, composed of a bottom gut culture chamber, an intermediate gas input layer, and a top layer containing the LED interface and Arduino microcontroller. The schematic illustrates the configuration of illumination ports, medium flow, and gas inputs for oxygenation. Stimulation protocols consist of 60 cycles of 10 s light (1 ms pulses at 2 Hz or 10 Hz) followed by 20 s pauses.

(b) Blueprint of LED array circuit design. Blue and yellow LED arrays are powered and controlled via an Arduino Uno board and custom software (supplementary data). Created in BioRender. Yissachar, N. (2025) https://biorender.com/5vgvgbv.

(c) Validation of pulse delivery at 1 Hz and 10 Hz, showing raw trace outputs and pulse detection. Raw data with the detected pulses. Pulses were administered at 1 and 10 Hz.

(d) Spectral profiles of yellow and blue LEDs, showing emission peaks at 570 nm and 450 nm, respectively, as expected.

Supplementary figure 2

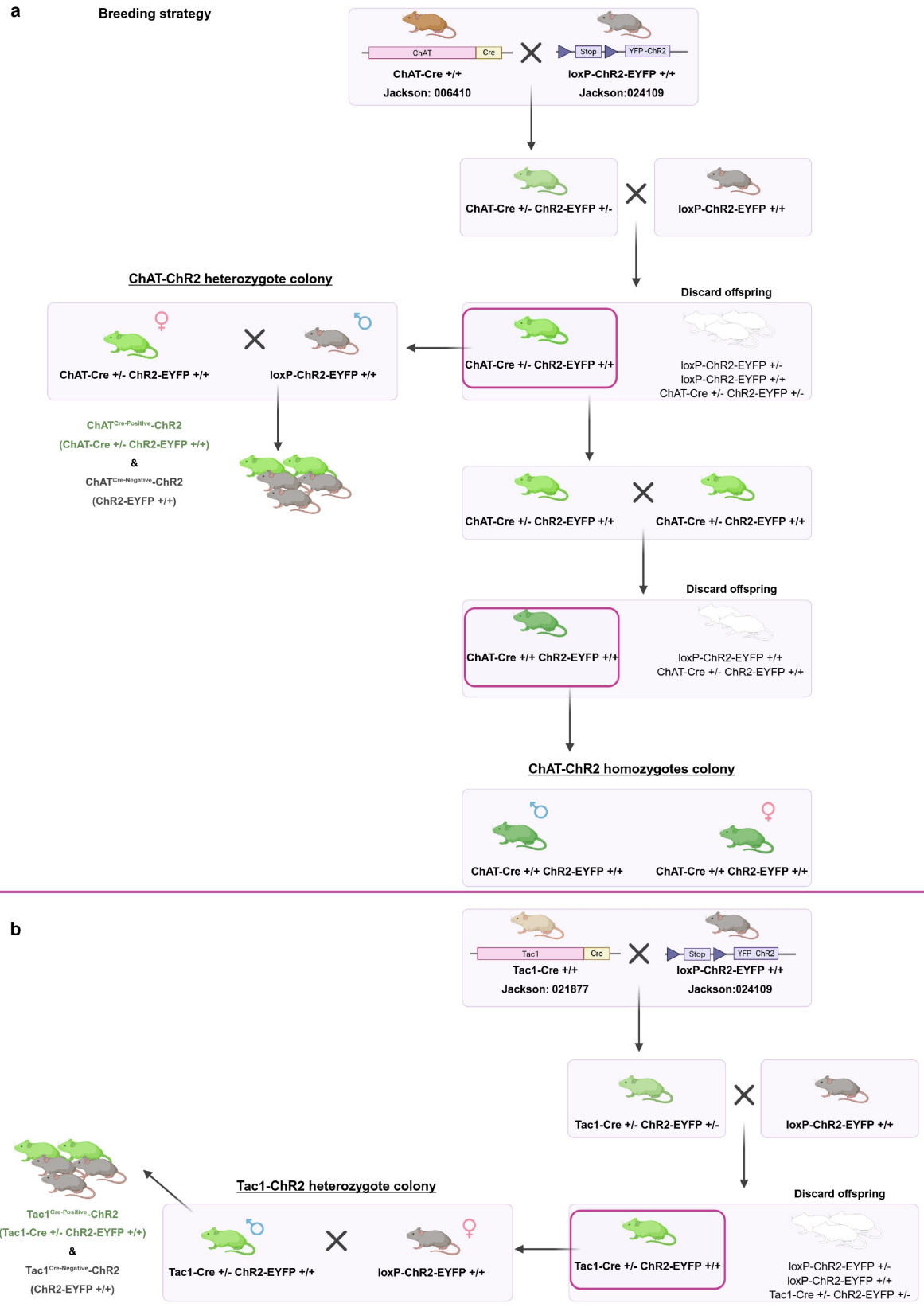

Supplementary Fig. 2: Breeding strategy for neuron-specific ChR2 expression

(a) Breeding strategy for generating *ChAT-Cre; ChR2-EYFP* mice. Crosses were performed to obtain either ChAT-ChR2 homozygous mice (*ChAT-Cre+/+; ChR2-EYFP+/+*) or ChAT-ChR2 heterozygous mice (*ChAT-Cre+/-; ChR2-EYFP+/+*). **(b)** Breeding strategy for generating Tac1-ChR2 heterozygous mice (*Tac1-Cre+/-; ChR2-EYFP+/+*). For all experimental, tissues were harvested from littermates that were ChR2-EYFP homozygous (ChR2+/+), differing only in the presence or absence of Cre recombinase (Cre+ vs. Cre−). Created in BioRender. Yissachar, N. (2025) https://biorender.com/nzv0htn.

Supplementary figure 3

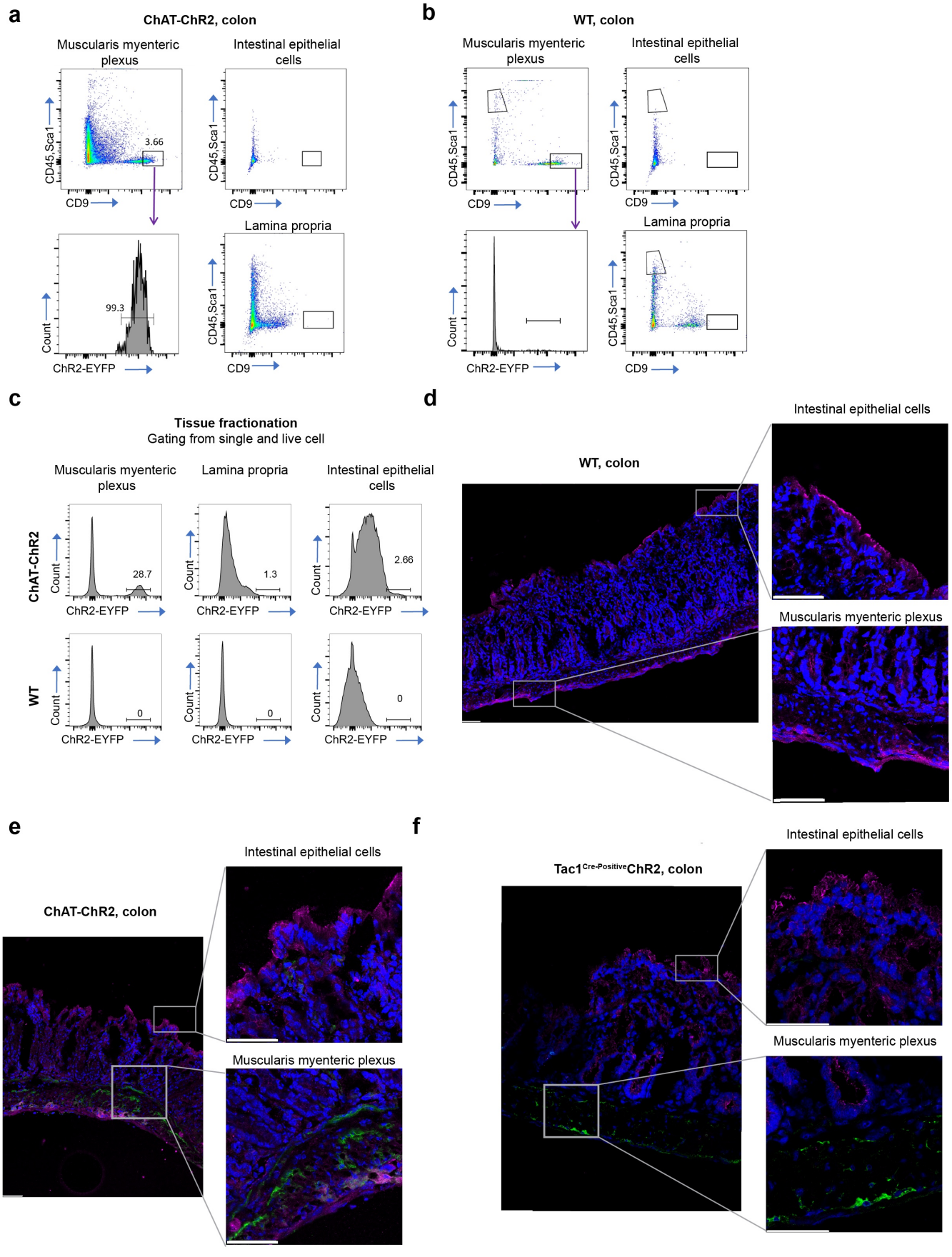

Supplementary Fig. 3: ChR2-EYFP expression in the ENS.

(a-b) Flow cytometry analysis of colon tissue compartments (myenteric plexus, epithelial layer, and lamina propria) from ChAT-ChR2 (a) or wild-type (WT) (b) mice. Cells were stained for CD45, Sca1, and CD9. EYFP+ ChAT-expressing enteric neurons ($CD45^{negative}Sca1^{negative},CD9^{high}$) were detected exclusively in the myenteric plexus of ChAT-ChR2 mice.

(c) Flow cytometry analysis of colon tissue compartments (myenteric plexus, epithelial layer, and lamina propria) from ChAT-ChR2 (top) or wild-type (WT) (bottom) mice. Histogram analysis shows ChR2-EYFP expression out of total, live, single cells extracted in each fraction.

(d-f) Representative confocal images of colon sections from WT (d), ChAT-ChR2 (e), and $Tac1^{Cre-Pos}$ChR2 (f) mice. Tissues were immunostained for epithelial markers (E-cadherin, magenta) and ChR2-EYFP (green); DAPI nuclear stain (blue). Scale bars: 50 μm.

Supplementary figure 4

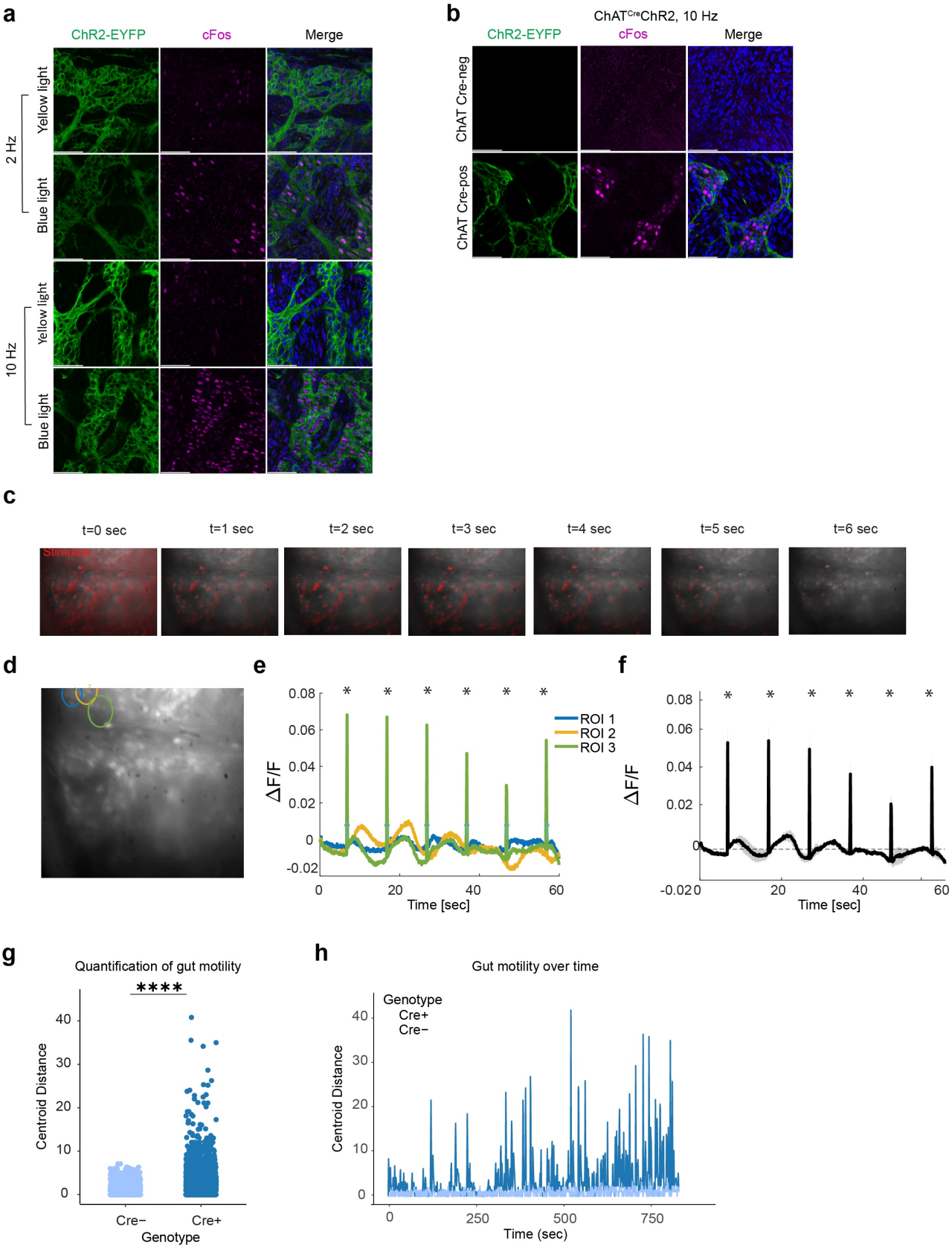

Supplementary Fig. 4: ENS activation following *ex vivo* optogenetic stimulation.

(a-b) Representative whole-mount images of colonic myenteric plexus after optogenetic stimulation of ChAT-ChR2 homozygous (a) or ChAT-Cre-positive/negative (b) tissues. Stained for cFos (magenta), ChR2-EYFP (green) and DAPI nuclear stain (blue); scale bar: 50 µm.

(c) Time-lapse frames from a representative field of view (FOV) showing fluorescence changes following a single 50 ms blue light pulse (t = 0 s). Calcium signal (red) is overlaid on the structural image of the tissue.

(d) Corresponding FOV with regions of interest (ROIs) demarcated, selected for quantification of calcium dynamics.

(e) Fluorescence traces (ΔF/F) from individual ROIs in (D), showing stimulus-induced calcium influx. Blue light pulse timing indicated by black asterisks.

(f) Averaged calcium response across all ROIs in (E). Baseline threshold (black dashed line) represents 2× the standard deviation of spontaneous activity during the initial 100 frames.

(g-h) Quantification of intestinal motility following optogenetic activation of ChAT-ChR2 neurons in the small intestine. (g) Centroid displacement per frame for individual samples, grouped by genotype: Cre^- (light blue) and Cre^+ (dark blue). Each point represents a single frame. ****$p < 0.0001$ by unpaired t-test. (h) Time-course analysis of gut displacement. Euclidean distance of the gut centroid was calculated at one-second intervals across two representative samples (Cre^+ and Cre^-). Each line represents a single intestinal sample.

Supplementary figure 5

a

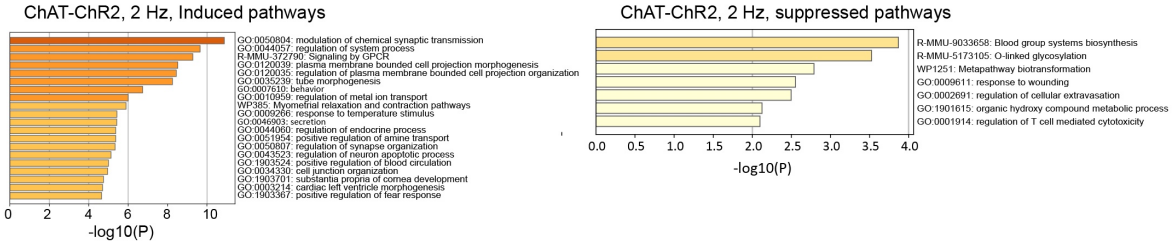

b

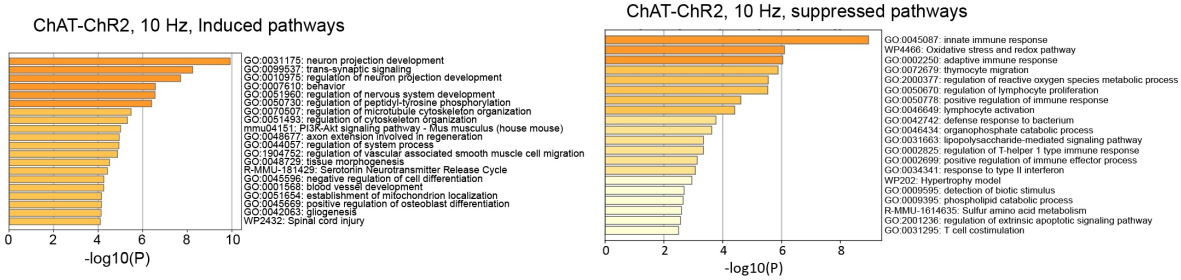

c

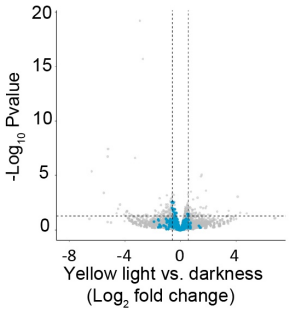

Supplementary Fig. 5: Transcriptional effects of optogenetic ChAT-ChR2 activation.

(a-b) Metascape pathway enrichment analysis of genes differentially expressed in ChAT-ChR2 tissues illuminated by blue vs. yellow light at 2 Hz (a) or 10 Hz (b) for 2 hr.

(c) Volcano plot comparing gene expression (RNAseq) in colon tissues exposed to yellow light vs. darkness. Genes induced by blue light compared to yellow light (per Fig. 2) are highlighted in blue.

Supplementary figure 6

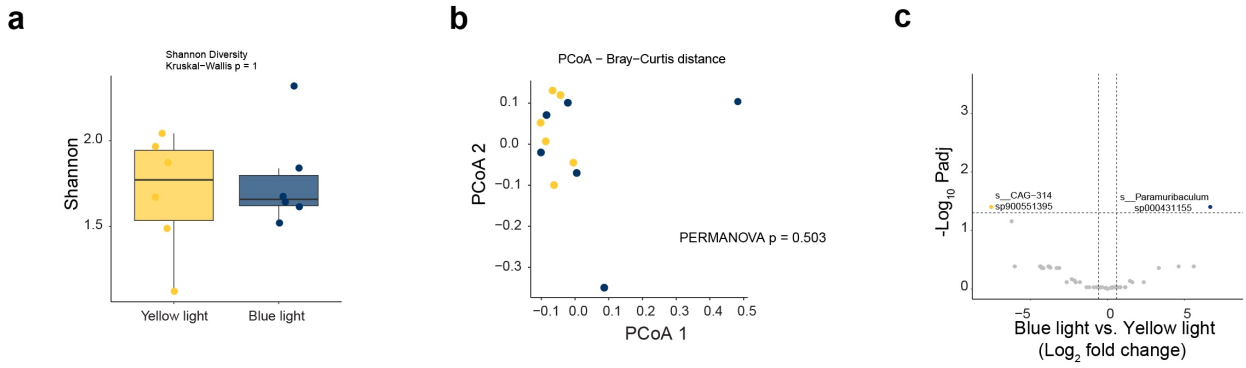

Supplementary Fig. 6: Microbiome composition following optogenetic stimulation of cultured ChAT-ChR2 colons

(a) Shannon diversity (α-diversity) calculated at the species level of colon microbiota from ChAT-ChR2 tissues exposed to 10 Hz blue (n = 6) or yellow light (n = 6); P = 1 by Kruskal–Wallis test.
(b) Principal coordinates analysis (PCoA) of Bray–Curtis distances based on species-level microbial profiles; PERMANOVA (999 permutations) p = 0.503. (n = 6 per condition).
(c) Volcano plot of differentially abundant taxa between blue- and yellow-light–illuminated tissues. Taxa with abs($\log_2$FC) ≥ 0.58 and adjusted p ≤ 0.1 are highlighted.

Supplementary figure 7

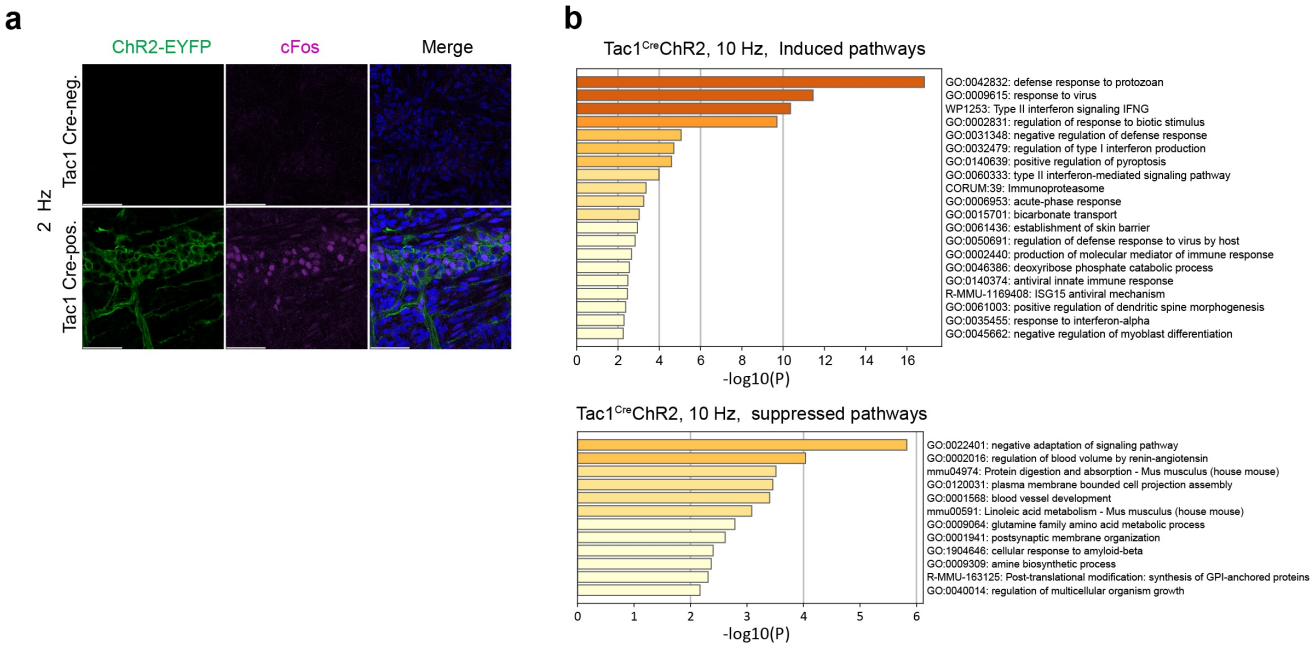

Supplementary Fig. 7: cFos activation and transcriptional responses in Tac1-ChR2 tissues.

(a) Representative cFos (magenta) and ChR2-EYFP (green) and DAPI nuclear stain (blue) staining in Tac1-ChR2 tissues illuminated with blue light (2 or 10 Hz); scale bar: 50 μm.

(b) Metascape pathway enrichment analysis of transcripts induced or suppressed by 10 Hz stimulation in Tac1-Cre-positive tissues (compared with Tac1-Cre-negative).

Supplementary figure 8

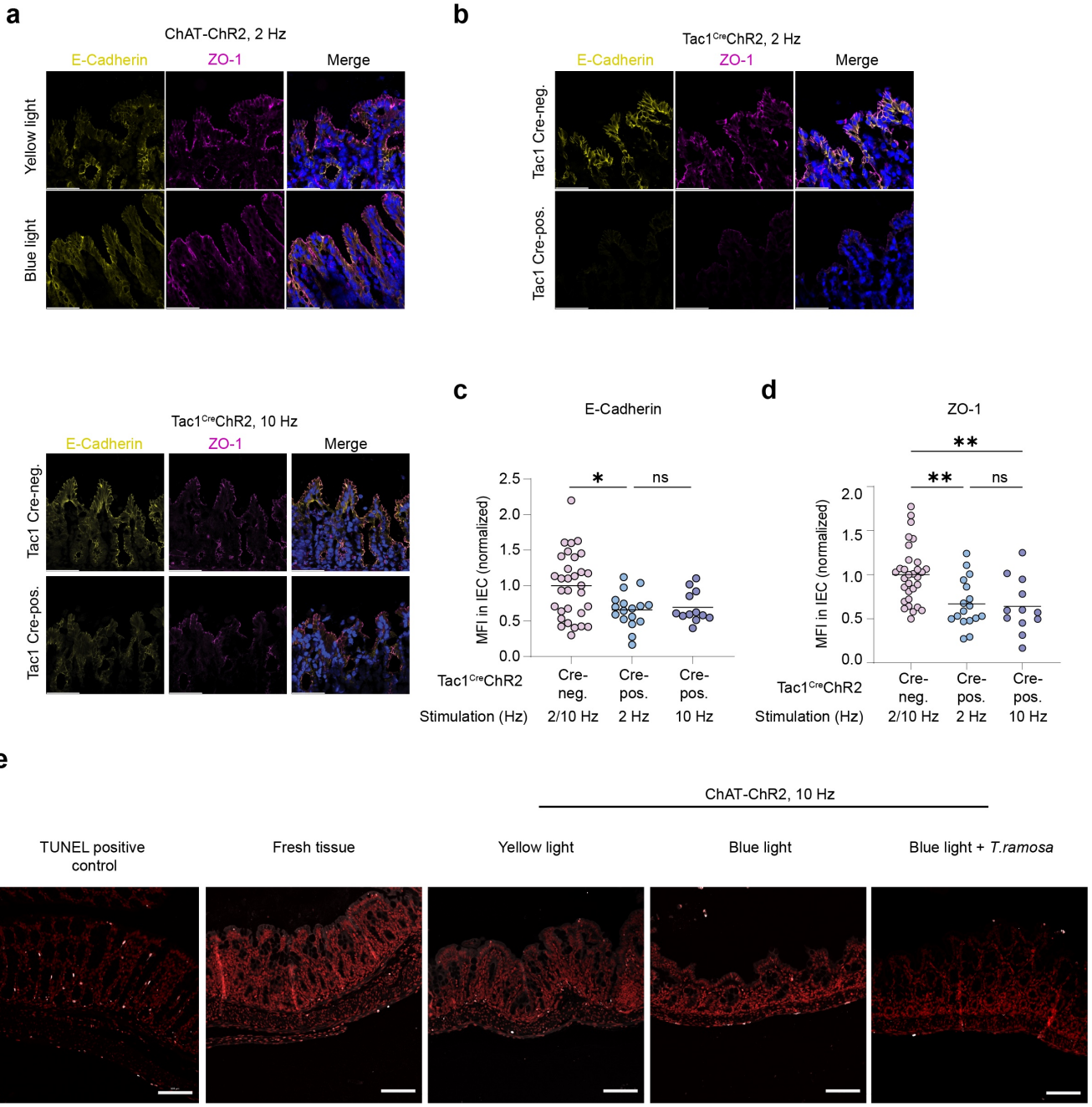

Supplementary Fig. 8: Tight junctions expression and epithelial viability following optogenetic stimulation.

(a-b) Representative Confocal images of ChAT-ChR2 (a) or $Tac1^{Cre}$ChR2 (b) tissues stained for E-cadherin (yellow), ZO-1 (magenta), and DAPI nuclear stain (blue). Scale bars: 50 μm.

(c-d) Quantification of E-cadherin (c) and ZO-1 (d) mean fluorescence intensity (MFI) in intestinal epithelial cells (acquired from 74 fields of view across 11 tissue samples). Statistical significance was determined by one-way ANOVA with multiple comparisons: *p = 0.0109, **p=0.0022 or 0.0033.

(e) Representative Confocal microscopy images for TUNEL staining of colon tissues post-stimulation, including positive control (10 Gy X-ray), fresh tissue, and tissues exposed to yellow or blue light (10 Hz) with or without luminal infusion of *T. ramosa*. Red: 7AAD; White: Br-dUTP. Scale bars: 100 μm.

Supplementary figure 9

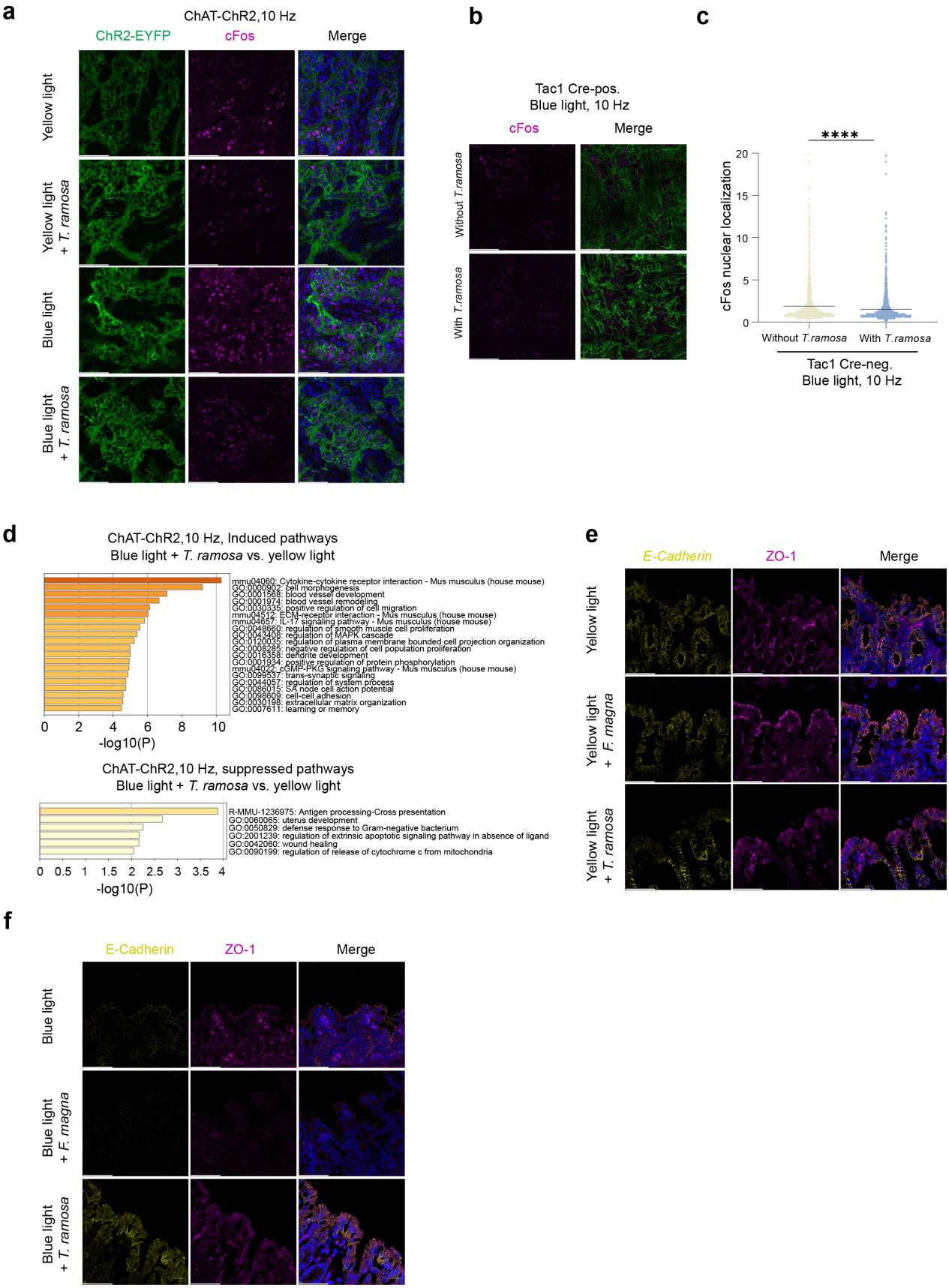

Supplementary Fig. 9: Gut microbes modulate neuronal cFos localization and ENS-driven transcriptional and barrier responses

(a) Representative whole-mount images of colonic myenteric plexus following ChAT-ChR2 stimulation (10 Hz) with or without luminal infusion of *T. ramosa*; cFos (magenta), ChR2-EYFP (green) and DAPI nuclear stain (blue); scale bar: 50 µm.

(b-c) Representative whole-mount staining images (b) and quantification (c) of cFos nuclear localization in Tac1$^{cre\text{-}pos}$ChR2 tissues stimulated with blue light (10 Hz, 2 hr in culture) with or without *T. ramose* (acquired from 51 fields of view across 6 tissue samples). ****P < 0.0001 by t-test. Scale bar: 50 µm.

(d) Metascape pathway enrichment analysis of transcripts induced or suppressed in ChAT-ChR2 tissues infused with *T. ramosa* and stimulated at 10 Hz vs. yellow light-illuminated tissues.

(e-f) Representative Confocal images of ChAT-ChR2 colon tissues infused with *F. magna* or *T. ramosa*, stained for E-cadherin (yellow), ZO-1 (magenta), and DAPI nuclear stain (blue), after stimulation with yellow (e) or blue (f) light (10 Hz, 2 hr in culture). Scale bar: 50 µm.